IAC-11-D1.4.11

A FRACTALLY FRACTIONATED SPACECRAFT

Giuliano Punzo
Department of Mechanical and Aerospace Engineering, University of Strathclyde, UK
giuliano.punzo@strath.ac.uk
Derek J. Bennet
Department of Mechanical and Aerospace Engineering, University of Strathclyde, UK,
derek.bennet@strath.ac.uk
Malcolm Macdonald
Department of Mechanical and Aerospace Engineering, University of Strathclyde, UK
malcolm.macdonald.102@strath.ac.uk

The advantages of decentralised multi-spacecraft architectures for many space applications are well understood. Distributed antennas represent popularly envisaged applications of such an architecture; these are composed of, typically, receiving elements carried on-board multiple spacecraft in precise formation. In this paper decentralised control, based on artificial potential functions, together with a fractal-like connection network, is used to produce autonomous and verifiable deployment and formation control of a swarm of spacecraft into a fractal-like pattern. The effect of using fractal-like routing of control data within the spacecraft generates complex formation shape patterns, while simultaneously reducing the amount of control information required to form such complex formation shapes. Furthermore, the techniques used ensures against swarm fragmentation, which can otherwise be a consequence of the non-uniform connectivity of the communication graph. In particular, the superposition of potential functions operating at multiple levels (single agents, subgroups of agents, groups of agents) according to a self-similar adjacency matrix produces a fractal-like final deployment with the same stability property on each scale. Results from the investigations carried out indicate the approach is feasible, whilst outlining its robustness characteristics, and versatility in formation deployment and control. Considering future high-precision formation flying and control capabilities, this paper considers, for the first time and as an example of a fractally fractionated spacecraft, a decentralised multi-spacecraft fractal shaped antenna. Furthermore, multi-spacecraft architecture exploiting fractal-like formations can be considered to investigate multi-scale phenomena in areas such as cosmic radiation and space plasma physics. Both numerical simulations and analytic treatment are presented, demonstrating the feasibility of deploying and controlling a fractionated fractal antenna in space through autonomous decentralised means.

This work frames the problem of architecture and tackles the one of control, whilst not neglecting actuation.

I. INTRODUCTION

Potential benefits disclosed by formation flight techniques for space science and remote sensing applications have been spotlighted since a while[1]. Traditionally the small number of spacecraft envisaged in formation flying concepts has been, in part, due to the complexity of simultaneously operating and managing a large number of independent spacecraft.[2] The problem thus becomes how to provide spacecraft, which are already autonomous with the additional capabilities required to perform collaborative tasks, such as precision relative positioning, while maintaining the desire to command a single entity.[3-4] This requirement has led to the popularisation of artificial potential functions (APF) based control method,[5-7] which can be used to gain an emergent group behaviour in agents without the need for a high-level on board intelligence. APF also gives the further advantage of providing a tractable control through stability.[5] Intuitively it can be understood that through global inter-agent interactions alone swarms of mobile agents can be made to crystallize in regular lattice configurations. These ones are scalable, and present intrinsic symmetry characteristics. Furthermore, the final pattern is homogeneous and typically does not require the positioning of individual agents, as agents autonomously select their relative positions driven by the artificial potential field. The drawback of this stands in the awkwardness in achieving complex patterns as different planar or three-dimensional lattices. Overcoming this was attempted and multiple levels of control were recentlyprosposed:[8-9] in this approach agents are grouped in smaller ensembles which maintain a cohesive behaviour by means of one agent for each group ensuring connectivity across different groups.

This paper investigates both the influence of a self-similar adjacency matrix and of asymmetric potential functions as a means to obtain self-similar patterns which then replicates at multiple levels providing both control for subgroups position and, indirectly, for orientation. Particular attention is put in showing how the change of a single parameter along the directed edges entering one node of the communication graph is

a condition sufficient to the emergence of a central symmetry in the pattern.

II. METHODOLOGY

An ensemble of N spacecraft is considered. This ensemble is divided in subgroups of n agents such that $N = n^k$ for some integer $k > 0$. The agents are connected according to a non-weighted non-directional graph described by the adjacency square matrix A of dimension N. The spacecraft are controlled through an APF that operates only along the edges of the graph with a pair-wise scheme. The spacecraft dynamics are described through the acceleration field $\ddot{x} = f(x, \dot{x})$ where idealised sensors and actuators are assumed. For the numerical integration performed, the initial positions are uniformly distributed within a spheres of given radius centred on the expected equilibrium final position as well as initial velocities in the corresponding velocity field. There is no global position or orientation of the final spacecraft formation but within the formation relative positions are considered for both spacecraft and groups of spacecraft, while relative orientation is considered only for groups of spacecraft. In section III it will be shown that it is possible to obtain a self-similar formation starting from mutually interacting agents. In the remainder of this section potential function characteristics and communication graph topology are described. For simplicity, planar configurations are considered but the same argumentations can be used in three dimensional formations. With reference to fractal terminology, the term "*initiator*" will be used to indicate the basic geometry of the formation composed of individual agents. The initiator is then propagated to group levels through the "*generator*". Here the difference between the two, in terms of formation, is just the level of control involved; i.e. there is no difference in the pattern but while the pattern of the initiators is composed of single agents, the pattern of generators is composed of groups of agents.

II.I Artificial Potential Functions

The spacecraft are controlled by artificial potential functions, in particular the Morse potential. This is composed of an attractive potential component (U_a) and a repulsive one (U_r), respectively defined as,

$$U_{ij}^{a} = -C_{aij} \exp\left(-\frac{\left|\vec{x}_{ij}\right|}{l_{aij}} \right)$$
$$U_{ij}^{r} = C_{rij} \exp\left(-\frac{\left|\vec{x}_{ij}\right|}{l_{rij}} \right) \qquad [1]$$

where, $C_{aij}, C_{rij}, l_{aij}$ and l_{rij} are constants whose values shape potential sensed by agent i because of interaction with agent j; $\vec{x}_{ij}$ is the relative position vector of agent i respect to agent j. The control law is completed by a virtual viscous-like damping in the form $\sigma \vec{v}_i$. This control law together with the hypothesis of no external disturbances and idealised sensing and actuation capabilities results in the following equation of motion,

$$\dot{x}_i = v_i$$
$$m\dot{v}_i = -a_{ij}\nabla_i U^a\left(x_{ij}\right) - a_{ij}\nabla_i U^r\left(x_{ij}\right) - \sigma v_i \qquad [2]$$

where

$$U_i^a = \sum_j a_{ij} U_{ij}^a$$
$$U_i^r = \sum_j a_{ij} U_{ij}^r \qquad [3]$$

and where, a_{ij} is the entry of the adjacency matrix as defined in section 2.2 and σ is a constant which provides a viscous damping effect.

II.II Self-similar Network

The network of interactions can be studied through graph theory, which makes use of the adjacency matrix. The adjacency matrix is a matrix that presents non-zero entries in the ij location whenever there is a directed edge from node i to node j that corresponds to a communication link between the two agents represented by nodes i and j. Moreover, the matrix is not weighted, meaning that only 0 or 1 entries are used, the "weight", i.e. the strength of the interactions is provided by the APF used. The adjacency matrix proposed is symmetric, hence the graph is not directed but this does not imply that the virtual interactions amongst the agents are symmetric. Artificial potential functions are not symmetric along every edge of the graph.

Edges belonging to fully connected n-agent groups form blocks along the main diagonal of the adjacency matrix. These can be regarded as initiators as defined previously, which are fully connected. In each group of n^2 nodes, groups of n nodes are linked through 4 directed edges. As 2 links between two distinct pairs of nodes in two groups are alone sufficient to uniquely define the relative orientation of the two groups of nodes, these links account for both relative position and orientation. Fig. 1 pictures the nonzero entries as dots for $n=5$ and $N=25$.

Extending this scheme to more agents it can be concluded that for any group of n^k agents for any integer

$k > 0$ the connections with groups of equal number of nodes are ensured through $2n^{k-1}$ nodes. Adjacency matrix for 125 agents is reported in Fig. 2.

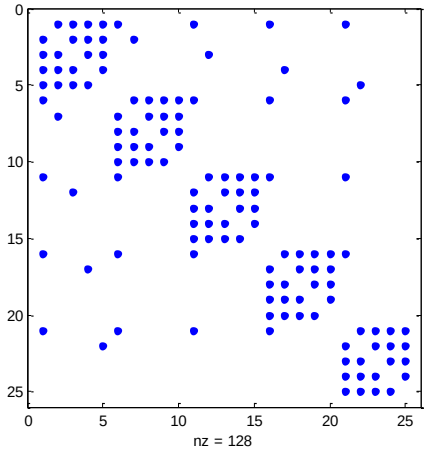

Fig. 1: Adjacency matrix for an ensemble of 25 nodes. Nonzero entries are represented by dots.

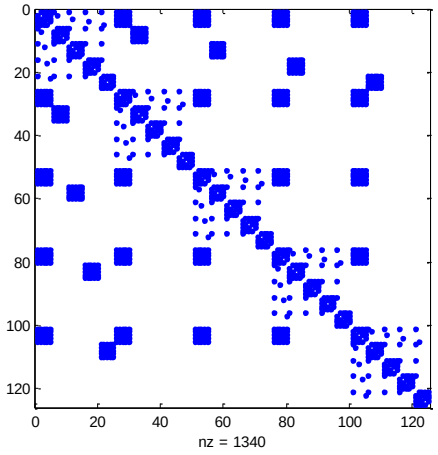

Fig. 2: Adjacency matrix for an ensemble of 125 nodes. The self-similarity of the matrix can be noticed.

This kind of network has the weakest part in the peripheral nodes. This means that loss control of one node due to loss of link is more likely for nodes that do not connect two levels but are just endpoints of their branch. This is advantageous as the loss of some links is more likely to produce the loss of a smaller portion of the network than of a large portion. Anyway each node is at least connected to 4 others and the most critical scenario is encountered for simultaneous loss of the two edges that link the initiator to the first generator in a configuration with just a generator. This would lead to the disconnection of a whole *n*-agent fully connected group. When the number of generators increases those groups which were end-points for the previous generator become embedded and more firmly bonded into the larger pattern. This ensures that in the most critical scenario the loss of at least 2 links is needed for the fragmentation to occur.

III. CONTROL LAW ANALYSIS

Control method applied to the spacecraft formation studied is based on APF as mentioned in Section II.I. In this section it is first shown how an asymmetry in attraction-repulsion potential leads necessarily to a central symmetry configuration. It is then shown how the APF coefficients are calculated in order to get the desired distance between agents. Finally nonlinear stability characteristics are drawn using total energy as Lyapunov function. **From now on just the case for *n=5* will be considered.**

III.I Central Symmetry Emergence

Central symmetry emerges at initiator level by means of asymmetry between the interactions of one single agent and the others at the same level. This is here explained by finding the conditions that make the artificial potential derivative null along two orthogonal axes centred on the agent considered. Considering the 5-agent scheme in Fig. 3 the first derivative of the artificial potential "sensed" by agent 2 can be calculated for the regular pentagon formation pictured*. Then the conditions that apply to the coefficients of the APF to be satisfied to get stable equilibrium are drawn. APF derivatives can be then derived from [4] for *i=1*.

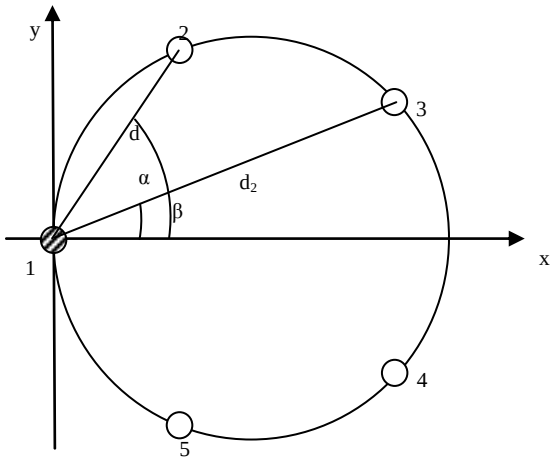

Fig. 3: 5-agent "pentagon" configuration. The shaded agent is the one which analysis refers to.

* Regular pentagon and in general regular polygon or solid shape emerge due to the fact that all the agents interact with the same strength, so no agent is supposed to be closer or further from the others

$$\frac{\partial U_i}{\partial x} = \sum_j \left(\frac{C_{aij}}{l_{aij}} \exp\left(\frac{\left|\vec{x}_{ij}\right|}{l_{aij}} \right) - \frac{C_{rij}}{l_{rij}} \exp\left(\frac{\left|\vec{x}_{ij}\right|}{l_{rij}} \right) \right) \frac{x_i - x_j}{\left|\vec{x}_{ij}\right|} \quad [4]$$

$$\frac{\partial U_i}{\partial y} = \sum_j \left(\frac{C_{aij}}{l_{aij}} \exp\left(\frac{\left|\vec{x}_{ij}\right|}{l_{aij}} \right) - \frac{C_{rij}}{l_{rij}} \exp\left(\frac{\left|\vec{x}_{ij}\right|}{l_{rij}} \right) \right) \frac{y_i - y_j}{\left|\vec{x}_{ij}\right|}$$

Excluding the trivial case for $l_{rij} = l_{aij}$ and $C_{rij} = C_{aij}$, Equations [4] can be made null while satisfying the stability conditions[6] $l_{rij} < l_{aij}$. From here on, just changes in l_{rij} parameter are considered while l_a, C_a and C_r are considered independent from the pair of agents *i-j* which they are referred to, that is, they take the same value for every *i,j* and it is assumed that the set of parameter used makes the APF a single minimum function, able to provide a stable behaviour. Taking the planar formation in fig. 4 the equilibrium along *y* is trivially satisfied for all possible distances *d* either in case $l_{rij} = l_r$ for all *ij*, that is it takes the same values along all the edges or in the case one agent has a different repulsive scale distance. This can be understood by simply considering the symmetry of the formation about *x*-axis.

Equilibrium along *x*-axis does not lead to an explicit expression for the equilibrium distance, nonetheless the expression

$$\frac{dU_1}{dx} = 2\frac{C_a}{l_a}\left(e^{\frac{-d_x}{l_a}} \cos(\alpha) + e^{\frac{-d_{2x}}{l_a}} \cos(\beta) \right) - 2\frac{C_r}{l_r^*}\left(e^{\frac{-d_x}{l_r^*}} \cos(\alpha) + e^{\frac{-d_{2x}}{l_r^*}} \cos(\beta) \right) \quad [5]$$

where,

$$d_{2x} = \frac{d_x}{2}\sqrt{\left(\tan(\alpha) + \frac{1}{\cos(\alpha)} \right)^2 + 1} \quad [6]$$

can be determined. Considering an initial equilibrium scenario in which agents are arranged as in Fig. 3for some equilibrium distance $d = d_x$ and for $l_r^* = l_r$ that is the same repulsive scale distance sensed by all the agents. In this scenario Equation [5] must return zero but if $l_r^* \neq l_r$ and in particular $l_r^* < l_r$ the separation distance must shrink, that is equilibrium distance shrinks as the scale separation distance shrinks. This can be verified by differentiating Equation [5] with respect to l_r^*. This returns

$$\frac{dU_1}{dx}\frac{dx}{dl_r^*} = 2\frac{C_r}{l_r^{*2}}\left(e^{\frac{-d_x}{l_r^*}} \cos(\alpha) + e^{\frac{-kd_x}{l_r^*}} \cos(\beta) \right) - 2\frac{C_r}{l_r^*}\left(\frac{d_x}{l_r^{*2}} e^{\frac{-d_x}{l_r^*}} \cos(\alpha) + \frac{d_x}{l_r^{*2}} e^{\frac{-kd_x}{l_r^*}} \cos(\beta) \right) \quad [7]$$

Expression [7] can be shown to be negative, that is verifying that a reduction of l_r^* produces an acceleration on agent 1 in the direction of positive *x*-axis, hence a reduction of its equilibrium distance:

$$2\frac{C_r}{l_r^{*2}}\left(e^{\frac{-d_x}{l_r^*}} \cos(\alpha) + e^{\frac{-kd_x}{l_r^*}} \cos(\beta) \right) - 2\frac{C_r}{l_r^*}\left(\frac{d_x}{l_r^{*2}} e^{\frac{-d_x}{l_r^*}} \cos(\alpha) + \frac{d_x}{l_r^{*2}} e^{\frac{-kd_x}{l_r^*}} \cos(\beta) \right) < 0$$
$$\therefore \left(\frac{d_x}{l_r^*} - 1 \right)\left(e^{\frac{-d_x}{l_r^*}} \cos(\alpha) + e^{\frac{-kd_x}{l_r^*}} \cos(\beta) \right) > 0 \quad [8]$$

This is always verified for $d_x > l_r^*$ as the second bracket is always positive. The condition $d_x > l_r^*$ can be obtained by a wide choice of system parameters as understandable by inspecting equilibrium distance for the simple case of two agents.

$$d = \frac{l_a l_r}{l_r - l_a} \ln\left(\frac{C_a l_r}{C_r l_a} \right) > l_r \quad [9]$$

In particular for $C_a = C_r$ this is verified as long as $l_a \neq l_r$, but as stability imposes $l_a > l_r$, to make the potential function convex, it can be concluded that this is always verified in this condition and possible to achieve for other choices of C_a and C_r parameters.

The other agents in the group considered, on the other hand tend to keep the same relative distance with respect to agent 1. This produces the new equilibrium configuration that sees the agent with reduced separation distance finding its equilibrium position in the centre of the 5-agent group while fulfilling also equilibrium conditions for the other agents. A contour plot of the potential which agent 1 senses is reported in Fig. 4 for both equilibrium and non-equilibrium parameter choice.

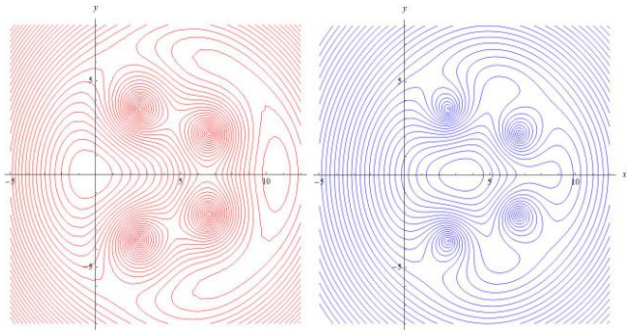

Fig. 4: Contour plot for artificial potential sensed by agent 1 in the origin. In case the scale repulsive distance is the same for all the agents an equilibrium at the origin is found (left). In case repulsive scale distance for of agent 1 is reduced (here halved) the equilibrium point moves towards the centre of the formation (right).

The same could be said for parameter C_r as the first Equations [4] is linear in C_r. Here anyway parameter l_r^* is used to force the central symmetry configuration over the pentagon one, while parameter C_r is used to produce the desired inter-agent distance only.

The cross configuration generated by the asymmetry in the potential repulsive scale length is sketched in Fig. 5.

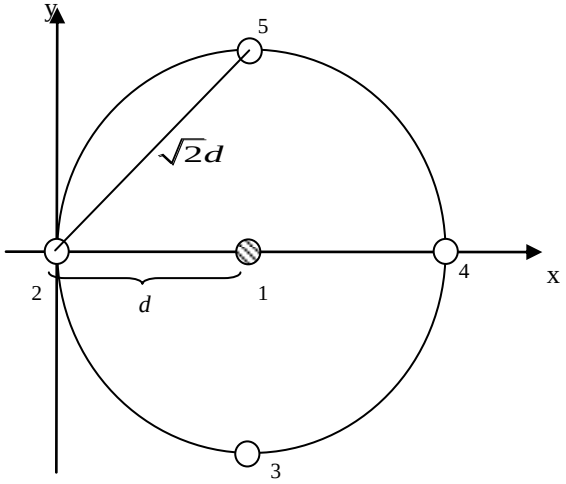

Fig. 5: Cross configuration for a 5-agent group. The shaded agent is the one with reduced repulsive scale distance.

Considering that interactions amongst agents are only along the edges of the adjacency matrix, a representation of the repulsive and attractive scale parameter as well as of the other coefficients playing into Equations [1] can be given in terms of matrix which have the same structure of the adjacency matrix described in Section II.II. An extract from repulsive distance matrix is reported in [10]

$$\begin{bmatrix} 0 & l_r & l_r & l_r & l_r & l_{r2} & 0 & 0 \\ l_r^* & 0 & l_r & l_r & l_r & 0 & l_{r3} & 0 \\ l_r^* & l_r & 0 & l_r & l_r & 0 & 0 & \cdots \\ l_r^* & l_r & l_r & 0 & l_r & 0 & \cdots & \cdots \\ l_r^* & l_r & l_r & l_r & 0 & 0 & \cdots & \cdots \\ l_{r2}^* & 0 & 0 & 0 & 0 & 0 & l_r & l_r \\ 0 & l_{r3} & 0 & \vdots & 0 & l_r^* & \ddots & l_r \\ \vdots & 0 & \vdots & \vdots & 0 & l_r^* & l_r & \ddots \end{bmatrix} \quad [10]$$

where, zeros are in the same positions as blanks in the adjacency matrix in Fig. 1 and Fig. 2, and where the coefficients regulating the interactions among nodes which are centres of two different 5-agent groups are denoted by l_{r2}. Finally l_{r3} is use to indicate the value along the edges connecting peripheral agents across different 5-agent groups.

Hence coefficients l_r, l_a, C_a and C_r can be arranged in square matrices of dimension *N* as they are referred to the edge and take a different value depending on which agents the edge connects.

Two considerations must hence be done:

a. Having $l_r^* = l_r$ does not imply that a 5-agent group will surely arrange itself into a pentagon configuration escaping the cross one. So while with l_r taking the same value across all the links, two configurations are possible, changing one single parameter along the edges exiting from one single agent will completely exclude the possibility of a circular formation. The latter may represent an unwanted outcome, or local minimum, of the self-arranging process.

b. Moreover in the pentagon formation proposed, in case $l_r^* = l_r$, calculating the potential sensed by one agent rather than another does not make any difference due to the central symmetry of the formation.

The second consideration does not apply when considering a cross configuration as in Fig. 5. Here the agent in the centre should be analysed too as its position cannot be considered as the one of any other agent in the group. Anyway it is in equilibrium whatever choice

of l_r parameter is done. This is due to the symmetry of potential acting on this agent which translates in two couples of equal and opposite terms for the sums in [4] making both equations trivially null. For this reason the agent with $l_r = l_r^*$ will find its equilibrium position at the centre enabling the cross formation. This also justify the first consideration as being the central position an equilibrium one, also a group of agents with the same repulsive potential can spontaneously arrange in a cross configuration.

Equilibrium for the surrounding agents according to the scheme of Fig. 5 is only determined by the first of the [4] as the *y*-component is null by symmetry. Equilibrium distance "*d*" as reported in Fig. 5 is found by finding values for "*d*" that satisfies

$$\frac{C_r}{l_r}\left(e^{\frac{-d}{l_r}}+e^{\frac{-2d}{l_r}}+\sqrt{2}e^{\frac{-\sqrt{2}d}{l_r}}\right)=\frac{C_a}{l_a}\left(e^{\frac{-d}{l_a}}+e^{\frac{-2d}{l_a}}+\sqrt{2}e^{\frac{-\sqrt{2}d}{l_a}}\right) \quad [11]$$

Which is obtained by expanding the first of Equations [4] for the present case. As it can be seen this is not solvable analytically. On the other hand, equilibrium can be found for a given "*d*", by tuning C_a and C_r parameters. This is better explained in the next paragraph.

III.II APF Coefficient Calculation

The coefficients of the APF acting along the edges of the graph are calculated such as to set the desired distance amongst the spacecraft. Later in this paragraph, the distance between agents is denoted as d_d to stress that this is a design distance and not an output of the definition of the control law. Moreover, the *ij* index will be dropped for practical purpose only. The C_r coefficient is calculated as a function of the others, which are set. The change of C_r parameter only or, more precisely, the change in the ratio C_r / C_a, is sufficient to modify the position of the minimum, hence the design distance, for the APF used. In particular, an interaction between two spacecraft belonging to two different *n*-agent groups is considered, with a design distance d_d; C_r coefficient can be hence calculated as

$$\frac{C_r}{C_a}=\frac{l_r}{l_a}e^{d_d\frac{l_r-l_a}{l_a l_r}} \quad [12]$$

Equation [12] can be reversed to calculate the equilibrium distance once the coefficients are set obtaining the right-hand side of Equation [9],

$$d_d=\frac{l_a l_r}{l_r-l_a}\ln\left(\frac{C_a l_r}{C_r l_a}\right) \quad [13]$$

When more than 2 agents are involved, an analytic expression for the equilibrium distance cannot be defined, but given a desired distance, an expression for the value of the ratio C_r / C_a can be produced to gain that separation. In particular for a fully connected group of 5 agents C_r / C_a ratio can be calculated equating to zero the gradient of the potential for the formation according to the scheme in Fig. 5. As the *y*-component is trivially null, C_r / C_a can be calculated considering just x-component of the gradient in Equation [4]. It is then possible to solve for C_r / C_a ratio and obtain

$$\frac{C_r}{C_a}=\frac{l_r}{l_a}\frac{e^{\frac{-d_d}{l_a}}+e^{\frac{-2d_d}{l_a}}+\sqrt{2}e^{\frac{-\sqrt{2}d_d}{l_a}}}{e^{\frac{-d_d}{l_r}}+e^{\frac{-2d_d}{l_r}}+\sqrt{2}e^{\frac{-\sqrt{2}d_d}{l_r}}} \quad [14]$$

This tuning method can be extended to the other links of the adjacency matrix defining so the coefficients to produce the desired self-similar pattern.

III.III APF Stability

Control law used can be proven to present non-linear stability characteristics. This is done here by considering a non-negative Lyapunov-like function and proving that its time derivative is everywhere negative except at equilibrium where it is required to be null.

Let's take to this end the total energy of the system *E* given by the virtual potential energy *U* and real kinematic energy *T*;

$$\frac{dE}{dt}=\frac{d(T+U)}{dt}=\frac{d}{dt}\left(\frac{1}{2}\sum_i^N m_i v_i^2+\frac{1}{2}\sum_i^N\sum_j^N a_{ij}U_{ij}\right)= \quad [15]$$
$$=\sum_i^N\left(m_i v_i\frac{dv_i}{dt}+\sum_j^N\left(a_{ij}\frac{dU_{ij}^a}{dt}+a_{ij}\frac{dU_{ij}^r}{dt}\right)\right)$$

Substituting [2]

$$\sum_i^N v_i\left(\sum_j^N\left(-a_{ij}\nabla U_{ij}^a-a_{ij}\nabla U_{ij}^r\right)-\sigma v_i\right)+\sum_i^N\sum_j^N\left(a_{ij}\frac{dU_{ij}^a}{dt}+a_{ij}\frac{dU_{ij}^r}{dt}\right)=$$
$$=\sum_i^N v_i\left(\left(-\nabla U_i^a-\nabla U_i^r\right)-\sigma v_i\right)+\sum_i^N\left(\frac{dU_i^a}{dt}+\frac{dU_i^r}{dt}\right)= \quad [16]$$
$$=\sum_i^N v_i\left(\left(-\nabla U_i^a-\nabla U_i^r\right)-\sigma v_i\right)+\sum_i^N v_i\left(\nabla U_i^a+\nabla U_i^r\right)=$$
$$=\sum_i^N -\sigma v_i^2\le 0$$

Hence total energy is an always decreasing function, that is, the ensemble will leak energy and stabilise

eventually into a static formation which corresponds to the minimum of total energy. As requested the chosen function is zero at equilibrium, that is characterised by having the speed of the spacecraft null. This of course does not consider the orbital speed in case of spacecrafts but just the speed calculated in an orbiting reference frame.

By very similar arguments it is possible to show how the total angular momentum is an exponentially decreasing function of time. By following the same procedure that applies to all-to-all connected ensembles[10] the total angular momentum derivative is calculated as

$$\frac{d}{dt}\sum_i\left(\vec{x}_i\times m\dot{\vec{x}}_i\right)=\sum_i\left(\dot{\vec{x}}_i\times m\dot{\vec{x}}_i\right)+\sum_i\left(\vec{x}_i\times m\ddot{\vec{x}}_i\right)= \quad [17]$$

$$=\sum_i\left(\vec{x}_i\times m\ddot{\vec{x}}_i\right)$$

Substituting [2]

$$\sum_i\left(\vec{x}_i\times m\ddot{\vec{x}}_i\right)= \quad [18]$$

$$=-\sum_i\left(\vec{x}_i\times\left(\nabla U_i^a+\nabla U_i^r\right)\right)-\sum_i\left(\vec{x}_i\times\sigma\dot{\vec{x}}_i\right)$$

The first sum is null because of symmetry of interactions, consequence of symmetry of adjacency matrix, so it can be concluded that

$$\frac{d}{dt}\sum_i\left(\vec{x}_i\times m\dot{\vec{x}}_i\right)=-\sum_i\left(\vec{x}_i\times\sigma\dot{\vec{x}}_i\right) \quad [19]$$

Hence, naming H the angular momentum

$$\frac{dH}{dt}=-\frac{\sigma}{m}H \quad [20]$$

that proves the exponential decay.

The stability characteristics just outlined does not imply that the system will relax into the desired formation as the energy might be minimized, even just in local sense, with a configuration that is not the one the system was meant to take.

IV. SIMULATION RESULTS

The control architecture presented was implemented in a numerical model simulating a swarm of spacecrafts arranging in fractal cross shape formations. Due to the limitation in memory for computation, simulations have been carried out for two formations of 25 and 125 spacecrafts, but orbital dynamics was considered just for the first one. As for the formation of 125 agents results can be considered valid in Lagrange L_1 environment. As for the 25 agent configuration a circular orbit was considered and Clohessi-Wilthshire[11] (CW) linearised equations were used. The orbiting reference system used has *x*-axis tangent to the orbit and parallel to orbital velocity vector, *y*-axis parallel to angular momentum vector and *z*-axis orthogonal to the first two and pointing towards the Earth centre. In this reference frame CW equations take form

$$\begin{aligned}\ddot{x}&=-2n\dot{z}\\ \ddot{y}&=-n^2y\\ \ddot{z}&=-2n\dot{x}-3n^2z\end{aligned} \quad [21]$$

where, n is the orbital frequency (the inverse of the orbital period).

Initial conditions for both cases were set such as each spacecraft had an initial position randomly selected within a sphere centred on its final position and radius equal to the distance to its nearest neighbour. This distance was set to be 1m; reasons leading to this choice are explained in details in section V. It is assumed that a carrier spacecraft or launcher releases the satellites with coarse accuracy although not completely randomly. The agent at the centre of the formation (say agent 1) is the only one linked to the centre of reference frame by a quadratic potential in the form $U_c=k\left|\vec{x}_1\right|^2$ with k as a weighting parameter set to 0.1. This is to provide a kind of orbit tracking capability or, in practical terms, the possibility to stay anchored to centre of the reference frame. Also this suggests that the task of tracking the orbit can be potentially carried out by one only agent, while the others just track their relative position with respect to the first one. This is not necessarily the one in the centre as it is done here for simplicity. The control law is applied for just *x* and *y* axis of the orbital reference frame with control on *z*-axis performed through a simple parabolic potential plus a dissipative term in the form $U_{zi}=k\left|\vec{z}_i\right|^2+\sigma\dot{\vec{z}}_i$, *for* $i=1\ldots N$, where, k and σ have the same roles and value as used previously, that flatten the formation on the plane $z=0$.

For the case of 25 spacecraft, of unit mass, the formation was deployed in a circular orbit with an altitude of 1000 km. For the case of 125 agents the connections between each group (consisting of 25 agents) are ensured by pairs of agents instead of groups of agents. This allows a reduction of the computational efforts for each agent and a reduction of the computational demand for the simulation. On the other hand this reduces the control power and slows down the deployment of the formation. Table 1 reports the value of the coefficients used.

	C_a	C_r	l_a	l_r
Fully connected groups	4	3.94722	2	1 l_r^*=0.5
Centres of f.c.g.	1	0.99596	4.5	4
Peripheral between adjacent f.c.g.	0.892521	1	2	0.5
Centres of 25-agent groups	1250	1252.66	10	9.9
Peripheral f.c.g. in 25 agent groups	34.98	35	3	2.9
				σ=0.1 for all the agents

Table 1: Coefficients for the APF used to control the formation

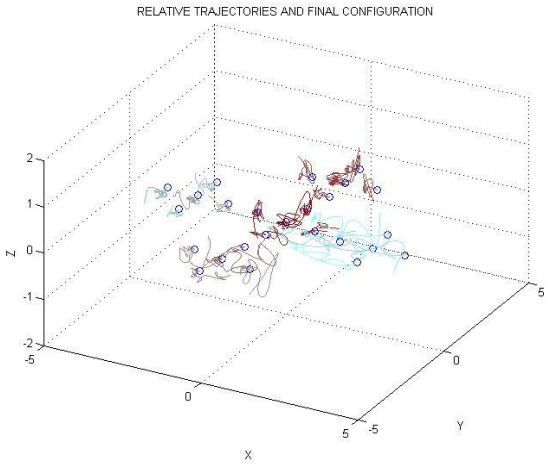

Fig. 6: Numerical simulation output - final pattern and trajectories. The formation is composed of 25 spacecrafts in 1000 km altitude circular Earth orbit. The plane of the formation is perpendicular to the orbit plane.

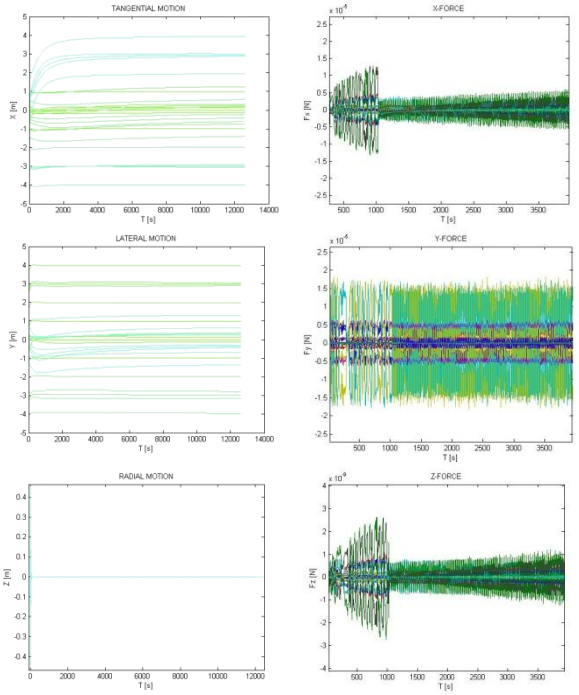

Fig. 7: Numerical simulation output – Motion and forces along the axes. The formation is composed of 25 spacecrafts in 1000 km altitude circular Earth orbit. The plane of the formation is perpendicular to the orbit plane.

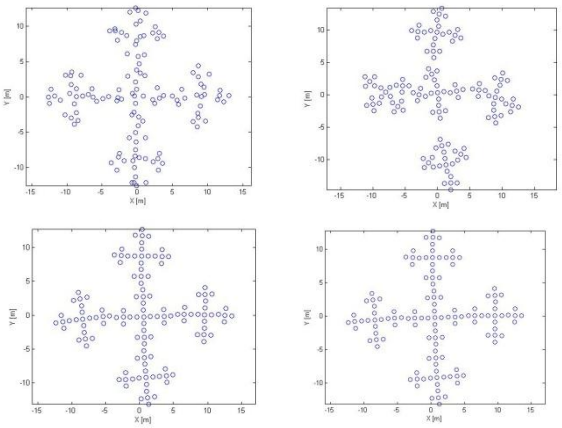

Fig. 8: Numerical simulation output – Snapshots from deployment of 125 agent formation at t=0 s (i), t=200 s (ii), t=30000 s (iii), t=160000 s (iv).

The slow pattern formation is mainly due to the elastic band effect that manifests when an ensemble of 25 agents is controlled by "pulling" one of them which is not rigidly linked to the others. The "virtual" links amongst agents are provided by APF which provide loose bonds, especially about the equilibrium position. It can be noticed how first small 5-agent groups form and then gather together in more structured formation.

V. DISCUSSION

Distances between spacecraft are designed to be with reference to the mission task. When spacecraft carry radio antenna designed to work as a distributed array, design distance depends on the wavelength used. Space based radio telescopes distributed on several spacecraft usually need for large separation distances (see for example Terrestrial Planet Finder Interferometer project[12]) while in case of perspective distributed antennas for telecommunications, inter-spacecraft distances would be in the order of metres or less. Considering the use of UHF that allow a good atmosphere penetration as well as not so short wavelength the separation distance between two spacecraft would not be larger than 50cm. This comes as the separation between two elements of a distributed array should not exceed $\lambda/2$. This suggests that such an application would be only suitable for small satellites and actuators using Lorentz forces or Coulomb forces.[13-14] and justifies the separation distance used in simulations, that was anyway doubled to further challenge system capabilities. Moreover the emergent fractal shape, which resembles the so-called "*Purina fractal*"[15] is expected to enhance exploitation of fractal antennas characteristics for distributed orbiting array defined.

Possible applications of the sensor network include, for example, ESA Cross Scale[16] or NASA Themis[17] mission, where the separation distance depends on the particular phenomenon that is being investigated.

One aspect that can be considered in the design of a spacecraft system is that a number of communication channels should be enabled to allow the fractal pattern to emerge, but these channels can be exploited for the communication needs amongst the different modules of a fractionated architecture beside control ones. For instance the guidance for the whole formation can be carried out by a number of spacecraft which communicate in an all-to-all scheme in order to share the computational efforts, and then passed to another module (possibly composed by more spacecraft) able to compare this to the navigation to eventually generate a control input for the whole formation. This is different from the GNC function that each spacecraft carries out: while each spacecraft should find its position in a distributed architecture, the whole system should follow a guidance law that enables the mission task achievement. The fractal communication network can be also exploited to allocate and distribute the computation tasks on several levels. Nodes in the fractal communication network can be grouped into different levels as either belonging to the *initiator* or to one of the *generators*. This sorting of the nodes can be used as base for the design of the computational architecture with agents on the same level carrying out tasks in parallel. For instance, referring to the 5-agent group based architecture described previously, peripheral fully connected groups can be assigned to a lower level computations with higher level carried out by central 5-agent group in each group of 25.

Finally, for what concerns simulation outputs, the persistency of oscillations, with consequent activation of the actuators, about the equilibrium position when the formation is deployed can be avoided at control level using a time varying value for the artificial viscosity and a threshold to the lowest sensor readings. It is anyway advisable to avoid thrusters as actuators with consequent reduction of plume impingement, especially in applications that require small separation distances, and fuel wasting due to oscillations. This suggests once again the use of Lorentz and Coulomb forces to control the formation.

VI. CONCLUSIONS

In this paper artificial potential functions and self-similar adjacency matrix are used to obtain self-similar patterns in a formation of autonomous mobile agents. The use of APF method enables an analytic development of the theory although some results can be shown just numerically. The system is cooled-down using artificial damping which, in terms of control, represent an improvable means as the dissipation of artificial potential energy may translate into real fuel waste for the actual spacecrafts.

Although the stability of the method can be analytically proved the risk of local minima is not excluded and as the number of links shrinks the eventuality of stacking in local minima gets higher. It is moreover to note that the connection scheme used accounts for at least double redundancy towards dispersion, that is any link between two agents can be lost without catastrophic consequences for the whole formation.

The emergence of self-similar, or fractal, patterns by combining APF and self-similar adjacency matrix can be exploited in space-based telecommunications and space science having benefits from the separation amongst the agents in the formation.

VII. FUTURE WORK

The present research will be further developed by assessing the feasibility and performances of actuation through electromagnetic forces (Coulomb and Lorentz) to control the formation and by considering possible reconfiguration manoeuvres. Comparison with low thrust electric actuator can be considered an asset. The case of elliptic orbits shall be included as well.

VIII.AKNOWLEDGMENT

The authors acknowledge the contribution of Mr Philippos Karagiannakis in the definition of the issues linked to the exploitation of the proposed architecture in the field of telecommunications.

[1] Leitner, J. Formation Flying: The Future of Remote Sensing from Space. (2004).

[2] Winfield, A. F. T., Harper, C. J. & Nembrini, J. in *SAB 2004 International Workshop, July 17, 2004 - July 17, 2004.* 126-142 (Springer Verlag).

[3] McInnes, C. R. Velocity field path-planning for single and multiple unmanned aerial vehicles. *Aeronautical Journal* **107**, 419-426 (2003).

[4] Barnes, E. A. & Bishop, B. E. Utilizing navigational capability to control cooperating robotic swarms in reconnaissance-based operations. *Proceedings of the 40th Southeastern Symposium on System Theory*, 338-342 (2008).

[5] Bennet, D. J. & McInnes, C. R. Verifiable control of a swarm of unmanned aerial vehicles. *Proceedings of the Institution of Mechanical Engineers, Part G: Journal of Aerospace Engineering* **223**, 939-953 (2009).

[6] McInnes, C. R. Vortex formation in swarms of interacting particles. *Physical Review E (Statistical, Nonlinear, and Soft Matter Physics)* **75**, 032904 (2007).

[7] D'Orsogna, M. R., Chuang, Y. L., Bertozzi, A. L. & Chayes, L. S. Self-Propelled Particles with Soft-Core Interactions: Patterns, Stability, and Collapse. *Physical Review Letters* **96**, 104302 (2006).

[8] Izzo, D. & Pettazzi, L. Autonomous and distributed motion planning for satellite swarm. *Journal of Guidance, Control, and Dynamics* **30**, 449-459 (2007).

[9] Sabatini, M., Reali, F. & Palmerini, G. B. Autonomous Behavioral Strategy and Optimal Centralized Guidance for On-Orbit Self Assembly. *Aerosp Conf Proc*, 2774-2785 (2009).

[10] Bennet, D. J., Biggs, J. & Macdonald, M. in *18th IFAC Symposium on Automatic Control in Aerospace* (Nara, Japan, 2010).

[11] Schaub, H. & Junkins, J. L. *Analytical mechanics of space systems*. (American Institute of Aeronautics and Astronautics ; London : Eurospan, 2003).

[12] Lawson, P. R. *et al.* Terrestrial planet finder interferometer 2006-2007 progress and plans - art. no. 669308. *P Soc Photo-Opt Ins* **6693**, 69308-69308 (2007).

[13] King *et al.* Vol. 19 *Journal of propulsion and power* 9 (American Institute of Aeronautics and Astronautics, Reston, VA, ETATS-UNIS, 2003).

[14] Peck, M. A., Streetman, B., M., S. C. & Lappas, V. Spacececraft Formation flying using Lorentz forces. *Journal of the British Interplanetary Society*, 263-267 (2007).

[15] Werner, D. H. & Mittra, R. in *Frontiers in Electromagnetics* 94-203 (Wiley-IEEE Press, 2000).

[16] ESA. Cross-Scale - Multi-scale coupling in space plasmas. (ESA, 2009).

[17] Bester, M. *et al.* THEMIS Operations. *Space Science Reviews*, doi:citeulike-article-id:3632576 (2008).